Published in Special Volume: "The 1999 Izmit and Duzce Earthquakes: Preliminary Results" Eds. A.Barka, O.Kozaci, S.Akyuz, and E.Altunel), ITU, Istanbul, 2000.

THE 1999 EARTHQUAKE SEQUENCE ALONG THE NORTH ANATOLIAN TRANSFORM AT THE JUNCTURE BETWEEN THE TWO MAIN RUPTURES

Leonardo Seeber[1]
John G. Armbruster[1]
Naside Ozer[2]
Mustafa Aktar[3]
Serif Baris[3]
David Okaya[4]
Yehuda Ben-Zion[4]
Ned Field[4]

1Lamont Doherty Earth Observatory of Columbia University, Palisades, NY 10964; <nano@ldeo.columbia.edu>
2The University of Istanbul, Geophysical Engineering Department, 34850, Avcilar, Istanbul
3Kandilli Observatory of Bogazici University, 81220, Cengelkoy, Istanbul
4University of Southern California, Los Angeles, CA 90089

Introduction

The Northern Anatolia fault system extends east-west for over 1600 km across Turkey and is one of the world's major fast-moving continental transforms, comparable to the San Andreas transform in California. The Anatolia block south of this transform moves west at about 24 mm/y relative to the Asian plate to the north (Reilinger et al., 1997). This motion is ascribed to the combined effects of north-south convergence between the Arabian and the Asian plates and subduction rollback in the Mediterranean (e.g., McClusky et al. 2000). Six distinct M7+ earthquake sequences have ruptured this boundary progressively from east to west beginning in 1939 (Barka and Kadinsky-Cade, 1988; Barka, 1996). The most recent and westernmost of these sequences occurred in 1999 and includes the Mw7.4 Izmit and Mw7.1 Duzce earthquakes. These two mainshocks ruptures were contiguous; they ruptured several distinct segments of the northern strand of the North Anatolia fault for about 160 km (e.g., Reilinger et al., 1999; Toksoz et al., 1999; Armijo et al., 1999; Hartleb et al., 1999). This sequence was very destructive in a large region of northwestern Turkey with many densely populated and industrialized areas, including parts of the city of Istanbul. The 1999 sequence may also have raised the likelihood of future large earthquakes in the "seismic gap" across the Marmara Sea which threatens more directly the Istanbul metropolitan area. It is also one of the best documented sequences to rupture a continental transform and may serve as a prototype of major earthquakes in other populated regions such as California. In this paper we present preliminary results obtained from a network of earthquake recorders covering the portion of the 1999 source zone near the juncture between the August 17 and the November 12 ruptures.

We refer to both M7+ events in 1999 as "mainshocks" because they were associated with clearly distinct aftershock sequences and fault ruptures. But these ruptures are contiguous and close in time so that the second "mainshock" could be considered an aftershock of the first one. Whether or not the second event is an "aftershock" is not just a matter of semantics, but reflects distinct hypotheses about the coupling between these large events. By considering both "mainshocks" to be in the same

sequence we wish to leave open a wide range of possibilities about the nature of this coupling. Preliminary results relevant to this issue are briefly addressed in this report.

The Karadere Seismic Network

The two mainshocks in 1999 ruptured several distinct segments of the northern strand of the North Anatolia fault (e.g., Reilinger et al., 1999; Toksoz et al., 1999; Armijo et al., 1999; Hartleb et al., 1999; Hartleb and Dolan, 2000). We operated a seismic network of 10 stations for almost half a year and a high-resolution 16-seismometer fault array at the center of the network for three weeks. Our network covered the 50-km-long Karadere segment, the eastern-most segment that ruptured in the first mainshock on August 17 with surface right-lateral displacement of 1-1.5 m (Figure 1). The Karadere segment strikes ENE and is expected to act as a restraining bend, like the Mojave section of the SAF. The reverse or thrust faulting in the focal mechanism of the Mw4.9 earthquake on 7/11/99 and the relatively high elevation (Figure 1) are consistent with this idea. The surface trace of the Karadere segment follows a narrow valley across a drainage divide where pre-Quaternary rocks are exposed. The rest of the August 17 rupture to the west surfaces through alluvial or submerged basins.

Our intermediate-spacing 10-station network along the Karadere segment was operative for about 5.5 months, from a week after the first mainshock to mid February 2000, or about three months after the second mainshock. During the last three weeks of the deployment, we operated a dense "T" array of 16 high-gain (L22) sensors in the middle of the network: 12 sensors in a ~0.7-km line across the August 17 rupture and 5 sensors in a ~1-km line along the fault. While the array was in place we augmented the network with an additional high-gain (L22) station to the east to improve our resolution on the sources for the array and detect fault-zone trapped waves at high resolution (e.g. , Ben-Zion, 1998).

All stations had REFTEK recorders operated in a triggered mode. They all recorded high-gain three component L22 sensors. In addition, all but two of the 10 long-term network stations recorded three strong-motion components from force-balance accelerometers (FBA). Stations MO (for the full deployment) and GE (only the first two months) recorded 3 broad-band components from Guralp CMG-40T (red symbols in Figure 1 mark stations operative for most of the deployment).

All sensors were installed near the ground surface and far from any above-ground structure. The broad-band sensor at station GE was mounted on bedrock. All other sensors were coupled to soil resting directly on bedrock, not on sediments in an active basin. All L22's and some of the FBA's (at BU, LS, TH, CL, CH, SL, and PO) were buried below the root mat. Other FBA's (at BV, VO, WF, FI, TW and FP) were fastened to buried wood blocks. This installation method allows the FBA's to be protected from moisture at the ground surface. Since the density of wood and soil are similar, the FBA is expected to remain coupled to the soil even in strong ground motion. The FBA at CH was installed in a small buried masonry tank empty of water. After the strong ground motion on November 12, none of the installations showed evidence of permanent deformation, either of the ground around the sensors or of the sensors relative to the ground, and all sensors were found to be still satisfactorily coupled to the ground.

Despite the particularly harsh 1999-2000 winter conditions in western Anatolia, the Karadere network was characterized by low-noise installations which operated nearly free of failures. Based on selective analysis of the data (Figure 2), we are confident that most of the 24K+ triggers coincident at 6 or more stations are earthquakes in the network area. About 1/3 of these events (7,745) were recorded by at least one FBA (Figure 3).The data from the Karadere network sample

thousands of sources spanning many orders of magnitude. They also sample at a range of distances across and along the fault zone. Near the fault zone ground motion was sampled in a tight array with 50-100 m spacing.

Aftershock Hypocenters and Seismogenic Depth Range

Preliminary analysis includes about 1000 hypocenter locations based on our data alone for subsets of earthquakes selected according to time, space, and size range. These hypocenters are based on a 1-dimensional velocity model given in Sellami et al.,1997. The epicenters are shown in Figure 2 where color coding refers to the time of the earthquakes. Only hypocenters with ERH and ERZ =<3.0km obtained by using HYPOINVERSE (Klein,1978) for 6 or more stations are shown in the cross-section (Figure 4). Higher resolution hypocenters are expected from a more complete analysis of our data in combination with data from other networks.

The hypocenters reported here are very preliminary, nevertheless they illuminate interesting structural detail, such as the Karadere fault steeply dipping to the north (Figure 4). The depth range of seismicity in this segment of the North Anatolia transform and along portions of the San Andreas transform are similar. The hypocenters illuminate brightly the Karadere segment over the depth range 8-14 km, but not above (Figure 4). Most of the hypocenters within range of the Karadere network are between 5 and 15 km deep (Figure 5). This remarkable lack of shallow aftershocks is reliable because our stations are distributed in the immediate vicinity of the rupture (Figures 1 and 2). Very few events recorded at these stations exhibit S-P times <1 sec. A lack of shallow seismicity has been noted in parts of the San Andreas transform, and has been ascribed to the fractured and weak nature of the crust in tectonically active environments (e.g., Scholz, 1999, p. 85). Tectonically stable continental regions produce relatively little seismicity, but much of it is concentrated in the upper 5 km of the crust (Seeber et al., 1996). This contrast in seismogenic depth range between active and inactive continental regions is relevant to the mechanical behavior of the crust, but also to hazard from earthquakes.

One important question is whether lack of shallow aftershocks is indicative of low radiated seismic energy in the same depth range of the mainshock rupture. Relatively weak radiation from the shallow depth is consistent with the surprisingly low peak acceleration (0.1g) from the November 12 mainshock recorded at our station BV which is located very close to the western terminus of that rupture (Figure 6). It is also consistent with apparent lack of particularly high damage in the immediate vicinity of the rupture, except for damage from dislocation along the rupture trace. Integration of this acceleration record in an attempt to recover the velocity and displacement histories (Figure 6) suggests complex and persistent long-period motion (5-10 seconds). The directivity of the first motion of the mainshock at BV is consistent with a nucleation point ˜15 km east of BV, as given by the Kandilli Observatory (Figure 1), and is similar to a much smaller aftershock (Figure 7). This energy may represent surface waves trapped in the Duzce basin (e.g., Frankel, 1993), but it could also reflect late- or post-seismic creep of the shallow portion of the rupture (e.g., Sharp and Saxton, 1989). This hypothesis is consistent with the relatively high energy level in the 3-10 seconds period for the first aftershock we have analyzed, 19 minutes after the mainshock (Figure 10a). Many other recordings are available during that time. This hypothesis may therefore be tested by systematically investigating all available data after the mainshock for long-period signal.

Secondary Faults

Small earthquakes stem from slip events on relatively small faults or fault patches. Large faults may be "illuminated" by small earthquakes if a sufficient number of such patches on that fault are represented as hypocenters. The ˜1000 hypocenters currently available from our network are primarily from before the 12 November mainshock. Most of these hypocenters are distributed in two broad clusters centered near the two geometric singularities marking the ends of the Karadere segment: the extensional gap and ˜15° bend at the northeastern end of the segment (and of the August 17 rupture); and the ˜20° bend and gap in the surface rupture at the southwestern end of the segment. A relatively small portion of the hypocenters are concentrated in a narrow tabular zone spatially associated with the Karadere segment (Figures 2 and 4). This correlation illustrates the resolution offered by the hypocenters. The sharp image of the fault is consistent with our claim of relative location accuracy of 1-3 km, depending on the distance from the network. Thus the broad clusters are real, they are not images of narrow zones distorted by poor locations. The seismicity sampled in Figure 2 is distributed across volumes between master strands of the North Anatolia transform; it is confined by these strands, but most of it is not on them. The internal structure of these broad clusters suggests complex systems of faults which, however, cannot be individually resolved from these preliminary results.

Our hypocenters suggest that many of the aftershocks originate from secondary faults, possibly cross faults straddling the volume between main strands. The concentration of these aftershocks near geometric complexities along the master faults is consistent with the notion that the secondary faults respond to stress concentrations near abrupt changes in the geometry and slip-distribution along the main rupture and contribute to the overall strain. We speculate, moreover, that they will show a wide variety of fault kinematics, just as regional focal mechanisms in western Turkey do (e.g., Dziewonski et al.,1981; Stein et al.,1997; Nalbant et al.,1998; Gurbuz et al., 2000). The Mw4.9 on 7/11/99 (Figure 1) is located close to the Karadere segment but its focal mechanism (Harvard) is inconsistent with right-lateral motion on this fault. While the seismogenic moment released by these faults may be small, a significant contribution to the total strain in the sequence is possible if they are slipping primarily by creep. Shallow dipping normal faults are often mapped in transtensional zones, but are rarely the sources of large earthquakes. Creep may be a particularly important mode of slip for these faults.

Near-Field Ground Motion of the November 12 Mainshock

Eight 3-component forced-balance accelerometers (FBA's) recorded on scale the ground motion of the Mw7.2 mainshock on November 12, 1999. The station parameters are listed in Table 1.

Table 1
FBA recordings of Mw7.1 November 12, 1999

STATION	PEAK ACC. (g)			DISTANCE
	Z	NS	EW	TO RUPTURE
BV	0.07	0.08	0.10	0.01? km
VO	0.19	0.89	0.51	10 km
FP	0.10	0.15	0.14	10 km
WF	0.06	0.16	0.12	14 km
FI	0.09	0.12	0.26	15 km
LS	0.05	0.10	0.13	17 km
CH	0.02	0.04	0.03	28 km
BU	0.02	0.03	0.05	31 km

Our recordings of the November 12 mainshock sample the near-field of this Mw7.2 (USGS) rupture in the along-strike quadrant westward from its western terminus (Figure 1). The closest recording is from this terminus; a ~30-cm scarp formed at a distance of about ten meters from the sensor at station BV. Peak accelerations at seven of our eight sites were small compared to the 0.8g peak acceleration recorded at Bolu (Figure 8) ~30 km east of the eastern terminus of the rupture. Peak accelerations in Karadere were also generally smaller than ones measured at similar distances for the M7.4 August 17 mainshock (Figure 8). These differences might be accounted for by source factors, such as magnitude, stress drop, rupture-propagation, and radiation pattern. Systematic differences in site response may also be a factor since the stations of the Karadere network were on bedrock and at least some of the other stations were not. It is critical to understand the nature of the large differences in peak ground motion recorded near the 1999 mainshocks (Figure 8).

Among the relatively low accelerations from the November 12 mainshock recorded by the Karadere network, station VO stands out as having recorded high acceleration, possibly the highest measured acceleration from either of the mainshocks (Figure 8). Site VO with 0.9g is on the surface trace of the Karadere segment, 10 km from the west terminus of the source (Figure 1). Only 400m from this site and 200m off the fault trace, peak acceleration recorded at station FP was 0.16g, five times lower (Figure 9). At another site on the trace of the Karadere segment 17 km from the source, however, peak acceleration was only 0.15g and was similar to peak accelerations away from the fault trace at a similar distance from the source (Figure 8). These measurements suggest that ground motion may be severely amplified along the fault zone, but only locally. A persistent high amplification at VO is suggested by the unusually large number of triggers at this station. Trigger for all FBA's were set at the same level, but he rate of triggers at VO is consistently about 2X the rate of triggers at either of the two companion stations =0.5 km from VO and the trace of the fault (FP or TW; Figure 3, note log scale). Spectral ratios for the on/off fault station pair VO/FP show similar large amplification at VO over a wide range of earthquake size, from M4.0 to M7.2 (Figure 10b). These preliminary results suggest that site condition is probably the main cause for the high acceleration at VO. Specific topographic and near-surface geologic conditions at the fault-zone site VO may play a critical role in the high acceleration. The data from the Karadere network samples thousands of sources spanning many magnitudes at a wide range of distances across and along the fault zone. These data are ideal for distinguishing the various factors thought to affect ground motion near the trace of a fault, such as fault-zone trapped waves, non-linear response, and amplification above topographic highs and near-surface low-velocity material.

Some of the preliminary results from the on/off fault station pair VO/FP suggest systematic dependency of amplification characteristics on the size of the source. Each of the spectral ratios for earthquake sources in Figure 10b have a broad ~x10 peak in the range 2-5 hz. These peaks seem to be systematically centered at lower frequency the larger is the earthquake. If these peaks reflect the same resonance, a shift to lower frequency for larger ground motion may reflect weakening of the subsurface material caused by the motion and a non-linear response (Joyner and Chen, 1975). This shift to lower frequency, however, is not combined with lower amplification factors (e.g., Field et al., 1998).

Another intriguing tentative observation is that the spectral ratio of the background noise sample just prior to the mainshock shows no evidence of relative amplification (Figure 10b). The x2-x3 peaks between 1-3 hz may not be significant (Field and Jacob, 1995). In contrast, the spectral ratio of "noise" 19 minutes after the mainshock shows significant peaks (Figure 10b). The second "noise" sample may contain signal from small earthquakes and so a possible interpretation is that only earthquake signals are amplified. Alternatively, the strong motion in the mainshock may have had a prolonged or permanent effect on the site characteristics. In line with this second hypothesis,

the onset of the P-wave at VO and FP from the main shock is remarkably similar in both shape and amplitude (Figure 8b). Half a second after the onset, the amplitude reaches 0.1g; shortly afterwards, the motion becomes incoherent and amplified at VO. A systematic survey of spectral ratios of earthquakes and noise before and after the mainshock would likely clarify this issue and possibly illustrate an interesting complex response at the fault-zone site VO.

Discussion: Seismo-Tectonic Setting of the 1999 Sequence.

Throughout its length, the North Anatolia transform tends to follow the pre-existing structural fabric inherited from the older collisional regime (Yilmaz et al., 1997; Okay et al., 1999; Yigitbas et al. 1999). In the central portion of the transform the relative plate-motion vectors appear to be parallel to the transform which, in turn, is parallel to the margin of the Black Sea and to older structure. The correlation between tectonic fabric and kinematics may account for the relatively simple behavior of this portion of the transform. The plate motion is almost entirely accounted for by a single fault strand and by relatively rare large ruptures. In contrast, the western portion of the transform is multibranched and is characterized by abundant background seismicity diffused in a broad swath. This complexity may be ascribed to divergence between the relative plate motion, which in northwestern Turkey is oriented east-southeast (Reilinger et al., 1997), and the east-west trending pre-existing structural fabric and passive margin. The plate boundary tends to follow the pre-existing fabric (e.g., Steckler and ten Brink, 1986) and consequently it is generally oblique to the relative motion vector in the Marmara region such that an extensional component must also be accommodated.

The transition from a relatively simple, narrow, and purely right-lateral to a complex, wide, and right-extensional boundary occurs near Bolu, where the North Anatolia fault undergoes the first of a series of westward bifurcations and is associated with a series of fault-controlled basins (Barka, 1996; Figure 1). The 1999 sequence ruptured the northern branch of this bifurcation for over 160 km. This sequence advanced westward the tip of the rupture in a secular progression and fits the compelling model of a series of mechanically interdependent ruptures (Stein et al., 1997; Nalbant et al., 1998). Similarly to some of the previous sequences in the series, however, the 1999 sequence complicates the picture in at least two interesting ways. First, the 1999 compound rupture nucleated in the Gulf of Izmit and propagated mostly eastward, in the opposite direction from the secular progression. The rupture reached as far as the Duzce basin on August 17 and on November 12 it continued to the east for another ~40 km (Figure 2). It appears to have stopped a few tens of km short of the bifurcation on the North Anatolia fault near Bolu. Secondly, the eastern half of this compound rupture overlapped the most recent ruptures, in 1957 and 1967. These ruptures were on the southern branch of the transform (Figure 1). Thus, a slip event on a strand of the plate boundary may not necessarily release stress and retard rupture on a parallel strand. Secondary faults may have a role in the coupling between parallel strands.

The moment released in the two main 1999 ruptures is almost completely right-lateral and has accounted for little or no extension (e.g., Reilinger et al., 1999; Toksoz et al., 1999; Armijo et al., 1999; Hartleb and Dolan, 2000; Figure 1). A significant component of extension over the long term is inferred from structural features, such as a series of active basins controlled by normal faulting from the Duzce basin to the Marmara. This suggests that the two components of strain are partitioned into distinct sets of faults, pure right-lateral and primarily normal, respectively. Conceivably, stress coupling between normal and strike-slip ruptures may account for some of the space-time complexity in rupture sequencing.

Conclusions

The following observations are based on a preliminary and partial set of hypocenters from a seismic network centered on the Karadere segment of the Duzce branch of the North Anatolia Transform during the 1999 earthquake sequence and pertain to that area only:

Seismicity is concentrated in a 10 km depth range and is characterized by a well defined upper limit. Very few earthquakes occur in the upper 5 km, even on the fault that ruptured to the surface in the mainshock.

Much of the seismicity in the 1999 sequence occurred on many secondary faults between strands of the North Anatolia fault system. The majority of the aftershocks do not stem from the faults responsible for most of the moment release.

In general observed peak accelerations for the Mw7.2 Nov 12, '99 mainshock are lower than expected, particularly for the station a few meters from the surface rupture. Ground motion however was severely amplified locally along the Karadere fault that ruptured on August 17, '99. Comparison of a station pair on/off this fault suggest systematic dependency of amplification characteristic on the size of the source and non-linear response of the fault zone.

Acknowledgments
Numerous public officials and private citizens contributed to the difficult task of maintaining a seismic network through the Anatolian winter. We are particularly indebted to Mr. Recep Altun, Mr. Hudyiet, Mr. and Mrs. Ozer and Mr. Ed Cranswick. NSF and SCEC provided funds for field expenses (EAR-8920136); IRIS/PASSCAL provided the instrumentation.

REFERENCES

Armijo, R., B. Meyer, A. Barka, J. De Chabaler and A. Hubert-Ferrari, The 1999 Izmit earthquake rupture and the tectonic evolution of the Sea of Marmara, abs. AGU December 1999.

Barka, A. A., and Kadinsky-Cade, Strike-slip fault geometry in Turkey and its influence on earthquake activity, Tectonophysics, 7, p.663-684, 1988.

Barka, A. A., Slip distribution along the North Anatolian Fault associated with large earthquakes of the period 1939 to 1967, Bull. Seis. Soc. Am., Vol.86, No.5, p.1238-1254, 1996.

Ben-Zion, Y., Properties of seismic fault zone waves and their utility for imaging low velocity structures, J. Geophys. Res., 103, 12567-12585, 1998.

Dziewonski, A.M., T.A. Chou and J.H. Woodhouse, Determination of earthquake source parameters from waveform data for studies of global and regional seismicity, J. Geophys. Res., 86, p.2825-2852.

Field E. H. and K. H. Jacob, a comparison and test of various site response estimation techniques, including three that are not reference site dependent, Bull. Seismol. Soc. Amer., 85, p.1127-1143, 1995.

Field, E. H., Y. Zeng, P. A. Johnson and I. A. Beresnev, Nonlinear sediment response during the 1994 Northridge earthquake: Observations and finite source simulations, J. Geophys. Res., 103, p.26869-26883, 1998.

Frankel, A., Three-dimensional simulations of ground motions in the San Bernardino valley, California, for hypothetical earthquakes on the San Andreas fault, Bull. Seismol. Soc. Amer., 83, p.1020-1041, 1993.

Gurbuz, C., M. Aktar, H. Eyidogan, A. Cisternas, H. Haessler, A. Barka, M. Ergin, N. Turkelli, O. Polat, S.B. Ucer, S. Kuleli, S. Baris, B. Kaypak, T. Bekler, E. Zor, F. Bicmen and A. Yoruk,

The seismotectonics of the Marmara Region(Turkey): results from a microseismic experiment, Tectonophysics, 316, p.1-17, 2000.

Hartleb, R. D., T. E. Dawson, A. Z. Tucker, J. F. Dolan, T. K. Rockwell, B. Terli, A. Dikbas, Z. Cakir, T. Gurer, O. Uslu and A. A. Barka, Surface rupture and slip distribution along the Duzce strand of the 17-August-1999 Izmit Turkey earthquake, abs. AGU December 1999.

Hartleb, R. D. and J.F. Dolan, Surface rupture mapping of the Karadere segment of the 17 August 1999 Izmit, Turkey earthquake and the western section of the 11 November 1999 Duzce, Turkey earthquake, Abstracts of the 95th Annual Meeting of Seismol. Soc. Amer., Seismological Res. Lett., Vol 71, N.2, p.223, 2000.

Hough, S.E., Empirical Green's function analysis: taking the next step, J. Geophys. Res. 102, p.5369-5384, 1997.

Joyner, W. B. and A. T. F. Chen, Calculation of non linear ground response in earthquakes, Bull. Seismol. Soc. Amer., 65, p.1315-1336, 1975.

Klein, W., Hypocenter location program HYPOINVERSE, USGS Open File Report 78-694, 1978.

McClusky, S. and 25 others, GPS constraints on crustal movements and deformations in the eastern Mediterranean (1988-1997): Implications for plate dynamics, preprint, 2000.

Nalbant, S.S., A. Hubert, G.C.P. King, Stress coupling between earthquakes in northwest Turkey and the north Aegean Sea, J. Geophys. Res., 103,B10, p.24469-24486,1998.

Okay, A., and O. Tuysuz, Tethyan sutures of northern Turkey, in : Durand, B., L. Jolivet, F. Horvath and M. Seranne eds., The Mediterranean basins : Tertiary extension within the Alpine orogen, Geological Society, London, Special Publications, 156, p.475-515, 1999.

Reilinger, R., A. Barka, R. Burgmann, A. Belgen, S. Ergintav, O. Gurkan, S. McClusky, H. Meteris, N. Toksoz, A. Turkezer, N. Yalcin and H. Yildiz, Coseismic slip for the August 17,1999, M=7.4 Izmit, Turkey earthquake from surface faulting and GPS measurements, abs. AGU December 1999.

Reilinger, R.E., S.C McClusky, M.B. Oral, R.W. King, M.N. Toksoz, A.A. Barka, I. Kinik, O. Lenk, and I. Sanli, Global Positioning System measurements of the present day crustal movements in the Arabia-Africa-Eurasia plate collision zone, J. Geophys. Res. 102, p.9983-9999, 1997.

Scholz, C, The mechanics of earthquakes and faulting, Cambridge University Press, New York, NY, 1999.

Seeber, L., G. Ekstrom, S. K. Jain, C. V. R. Murty, N. Chandak and J. G. Armbruster, The 1993 Killari earthquake in central India: A new fault in Mesozoic basalt flows?, J. Geophys. Res., 101, p.8643-8560, 1996.

Sellami, S., N. Pavoni, D. Mayer-Rosa, S. Mueller, H. Eyidogan, M. Aktar, C. Gurbuz, S. Baris, O. Polat and N. Yalcin, in Active Tectonics of Northwestern Anatolia-The Marmara Poly-Project, Eds. C. Schindler and M. Pfister, p. 449-486, v/dlf Hochschulverlag AG an der ETH Zurich, 570pages,1997.

Sharp, R. V. and J. L. Saxton, Three-dimensional records of surface displacement on the Superstition Hills fault associated with the earthquakes of 24 November 1987, Bull. Seismol. Soc. Amer., 79, p.376-389, 1989.

Stein, R.S., A.A. Barka, and J.H Dieterich, Progressive failure on the North Anatolian fault since 1989 by earthquake stress triggering, Geophys. J. Int. 128, p.594-604, 1997.

Steckler, M. S. and U.S. ten Brink, Lithospheric strength variations as a control on new plate boundaries : examples from the Arabian Plate, Earth. Planet. Sci. Lett., 79, p.120-132, 1986.

Toksoz, M. N., M. Edie, C. G. Doll, L. Xu, V. F. Cormier and M. Bouchon, Fault rupture process of the 17 August 1999 earthquake in Turkey, abs. AGU December 1999.

Yilmaz, Y., O. Tuysuz, E. Yigitbas, S.C. Genc, A.M.C. Sengor, Geology and tectonic evolution of the Pontides, in A.G.Robinson ed., Regional and petroleum geology of the Black Sea and surrounding region : AAPG Memoir 68, p.183-226, 1997.

Yigitbas, E., A. Elmas, Y. Yilmaz, Pre-Cenozoic tectono-stratigraphic components of the Western Pontides and their geological evolution, Geological Journal, 34, p.55-74, 1999.

FIGURES:

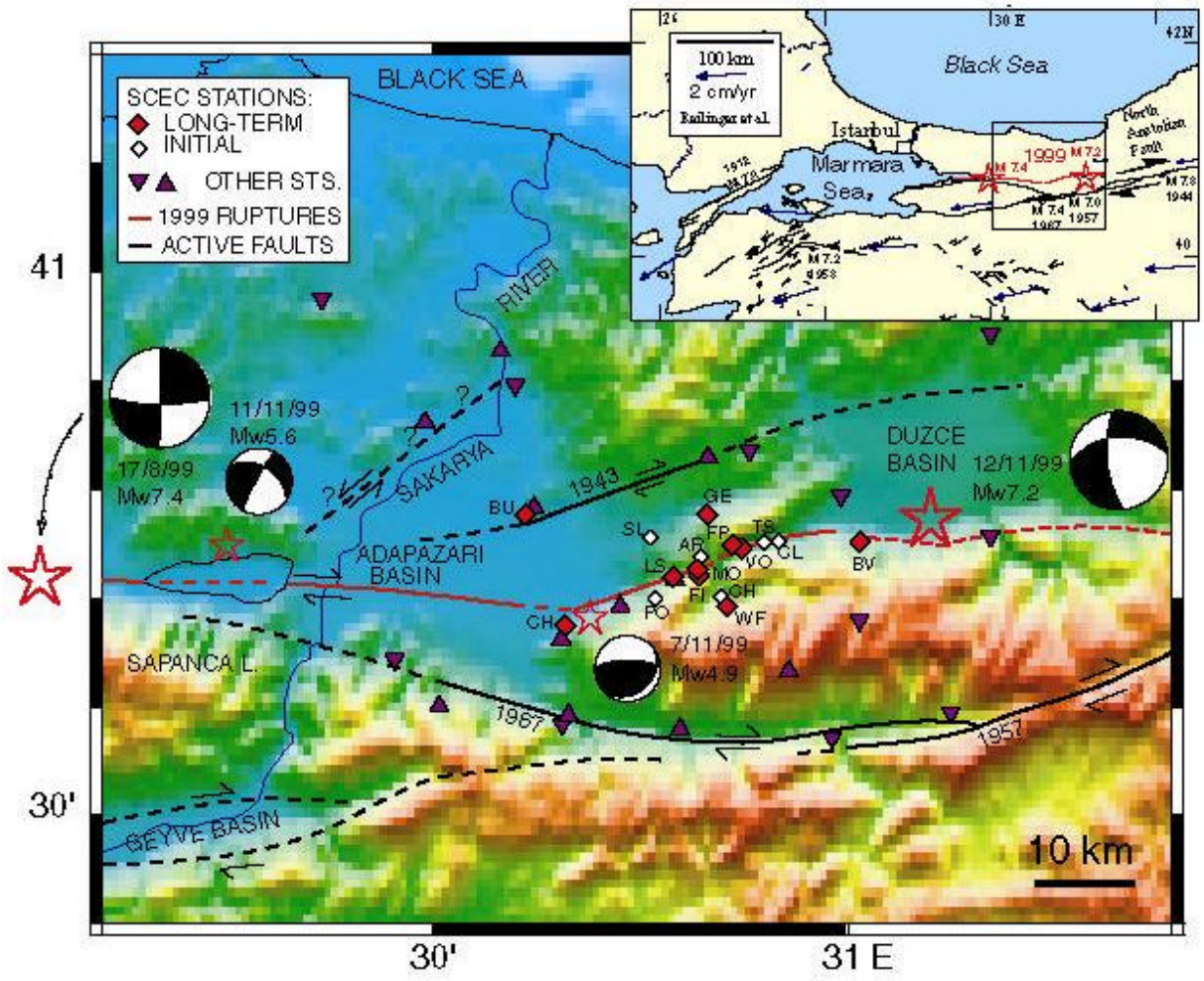

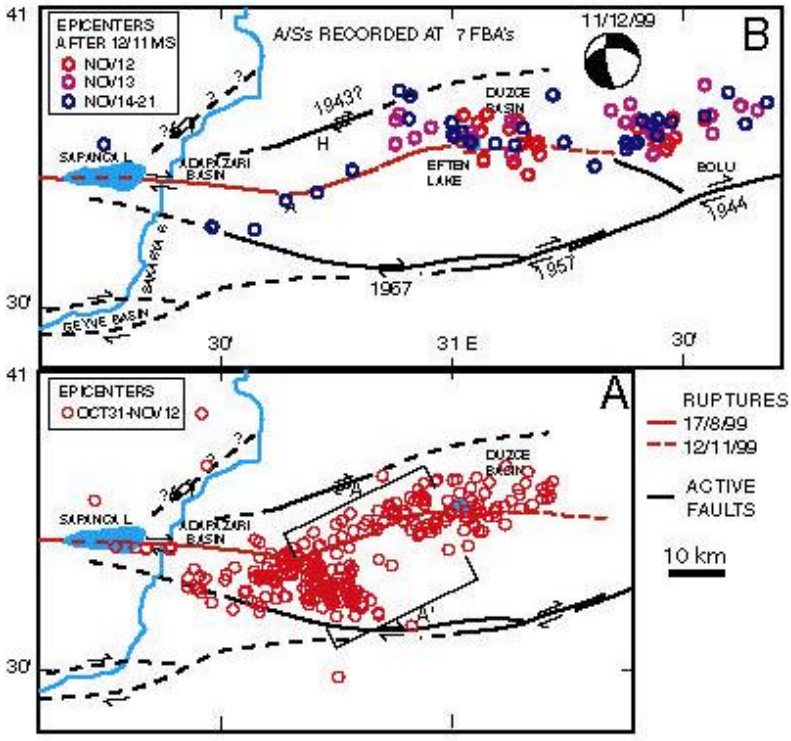

Figure 1. Study area in northwestern Turkey showing topography and main faults with time of latest ruptures. The 8/99 Izmit and 11/99 Duzce ruptures are in red: solid and dashed, respectively. Our 10-station network (white and red) covers the Karadere-Duzce segment of the rupture. White symbols represent stations that operated only in the initial deployment period (1 week). Red symbols represent stations deployed from the beginning of September '99 to February 15 '00. Stations operated by other groups are shown in purple.

Figure 2. Preliminary aftershock locations from the Karadere network (figure 1). Hypocenters are from samples of data before (A) and after (B) the Nov 12 Mw7.2 mainshock. The earthquakes in B are recorded by 7 FBAs and occurred within 9 days of the mainshock. They are color coded according to time after the mainshock. Aftershocks the first day (red) outline the November 12 mainshock rupture (dashed). The section AA' is in Figure 4. Hypocenters tend to fill volumes between the steep right-lateral strands of the North Anatolian Transform suggesting that many small earthquakes originate on secondary faults.

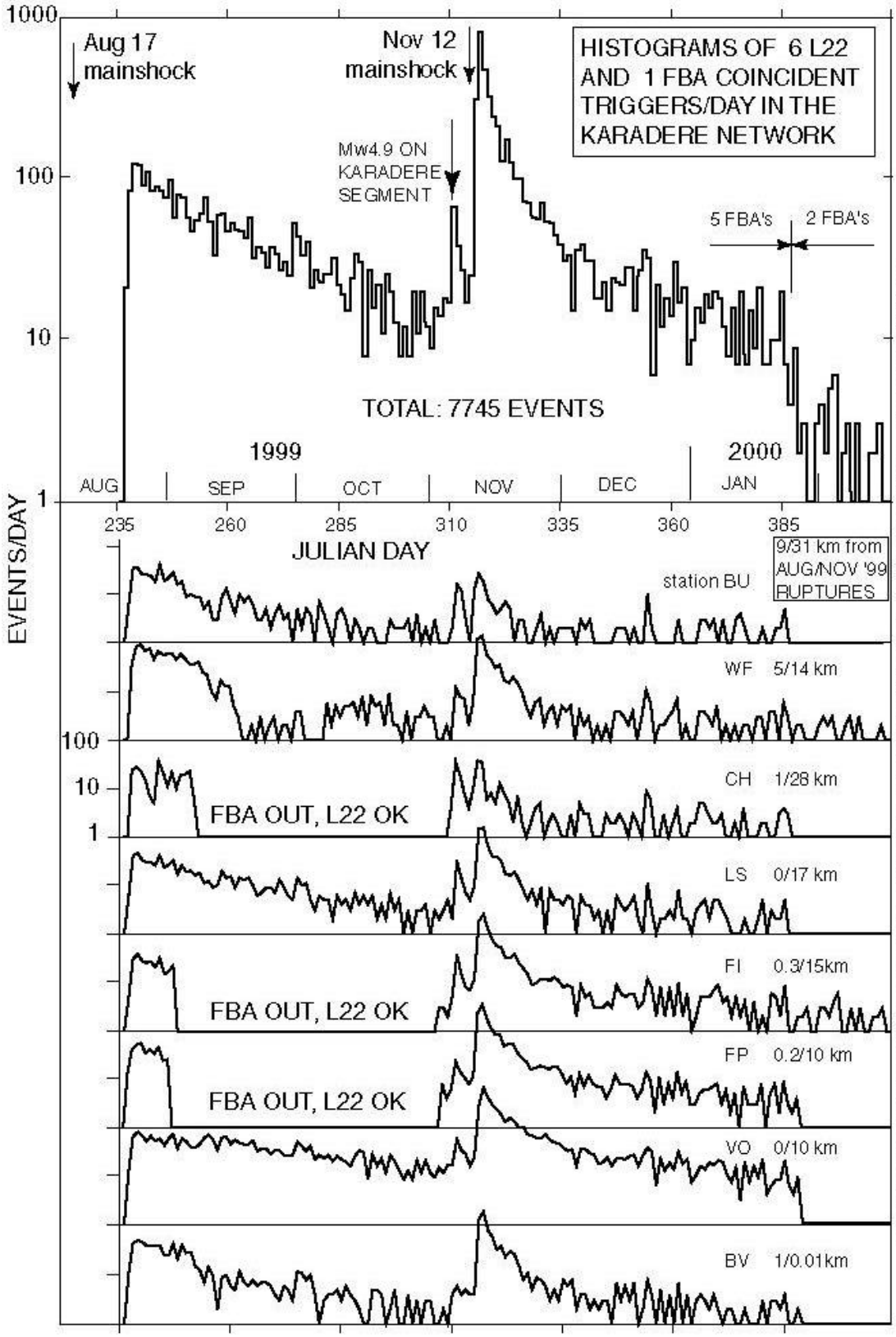

Figure 3. Histogram of the number of events which triggered within 5 seconds at least six L22 and at least one FBA in the Karadere network. These coincidence triggers are a conservative estimate of the local earthquakes recorded on at least one FBA. Note that the decay of aftershock activity is consistent with Omori's law (linear on a log scale) up to the end of October. The seismicity rises two weeks before the Nov 12 mainshock. L22 were operative at the three stations where FBA failed in September and October. L22's and a broad-band sensor were operative at two additional stations.

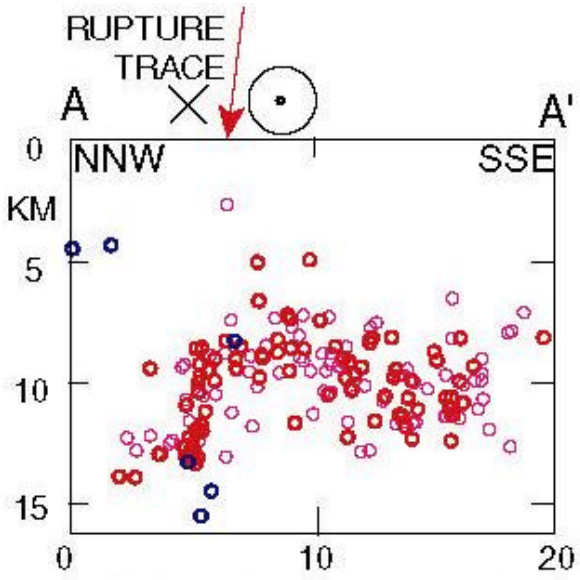

Figure 4. Vertical section showing hypocenters across the western portion of the Karadere segment (located in Figure2A).

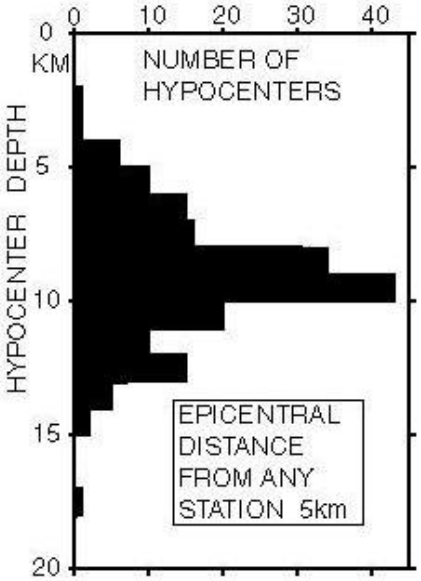

Figure 5. Depth distribution of hypocenters in the vicinity of the Karadere network.

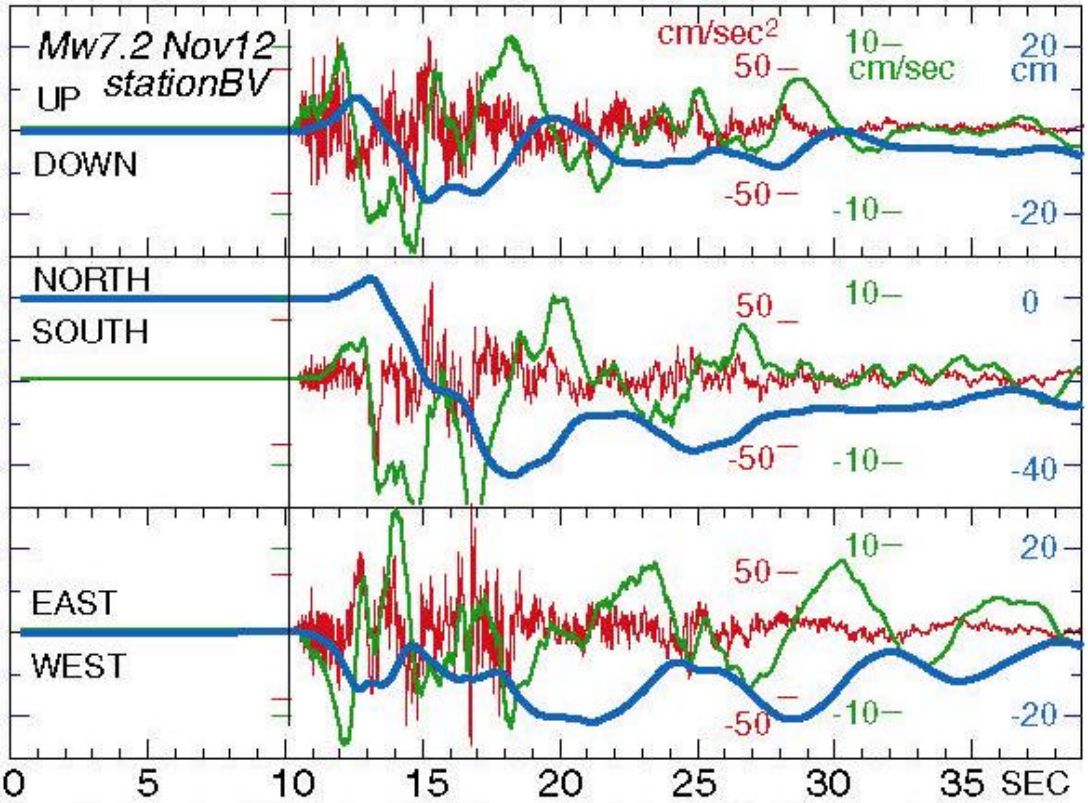

Figure 6. November 12 mainshock Mw7.2 recorded at station BV which is located 10 m from a surface scarp with 30-40cm displacement at the western terminus of the surface rupture. The FBA acceleration record (red) has been integrated once (green) and then again (blue) trying to infer the velocity and displacement histories.

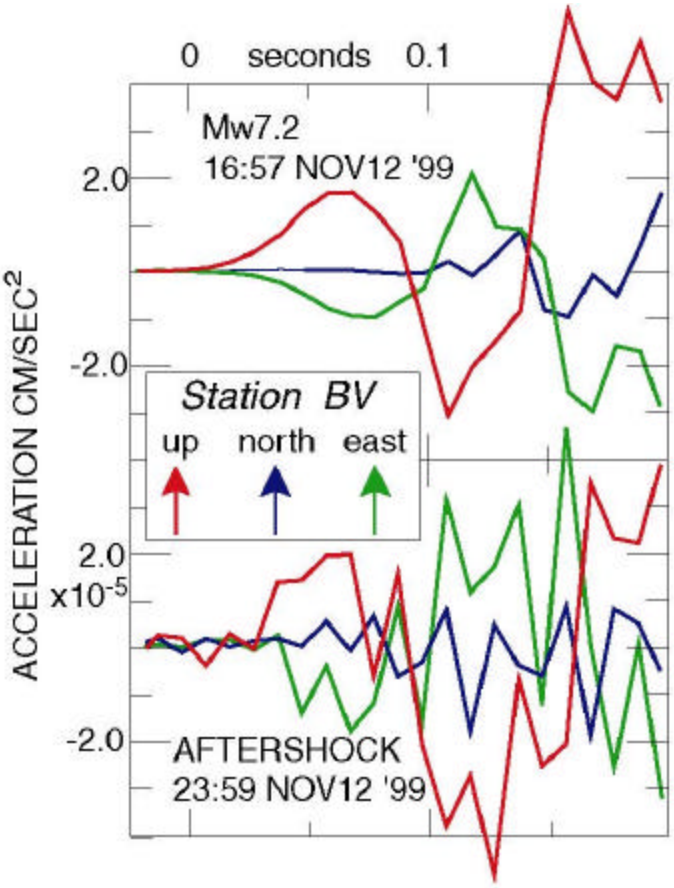

Figure 7. P-wave onset for the M7.2 Nov 12 '99 mainshock and for a small early aftershock recorded by FBA at station BV. This station is 10m from a surface scarp near the western end of the mainshock rupture. Waveforms are similar, suggesting similar source locations (east of BV), but amplitudes are different by 10^5.

Figure 8. Comparison of FBA acceleration records at stations VO and FP, both about 10 km from the nearest point on the source. Station VO is located on the Karadere segment of the August 17 rupture; station FP is 200 m from this fault and 400 m from VO. The large overall difference in the N-S motion, is contrasted by the remarkable similarity of the vertical components of motion in the first 1/2 second of the P-wave.

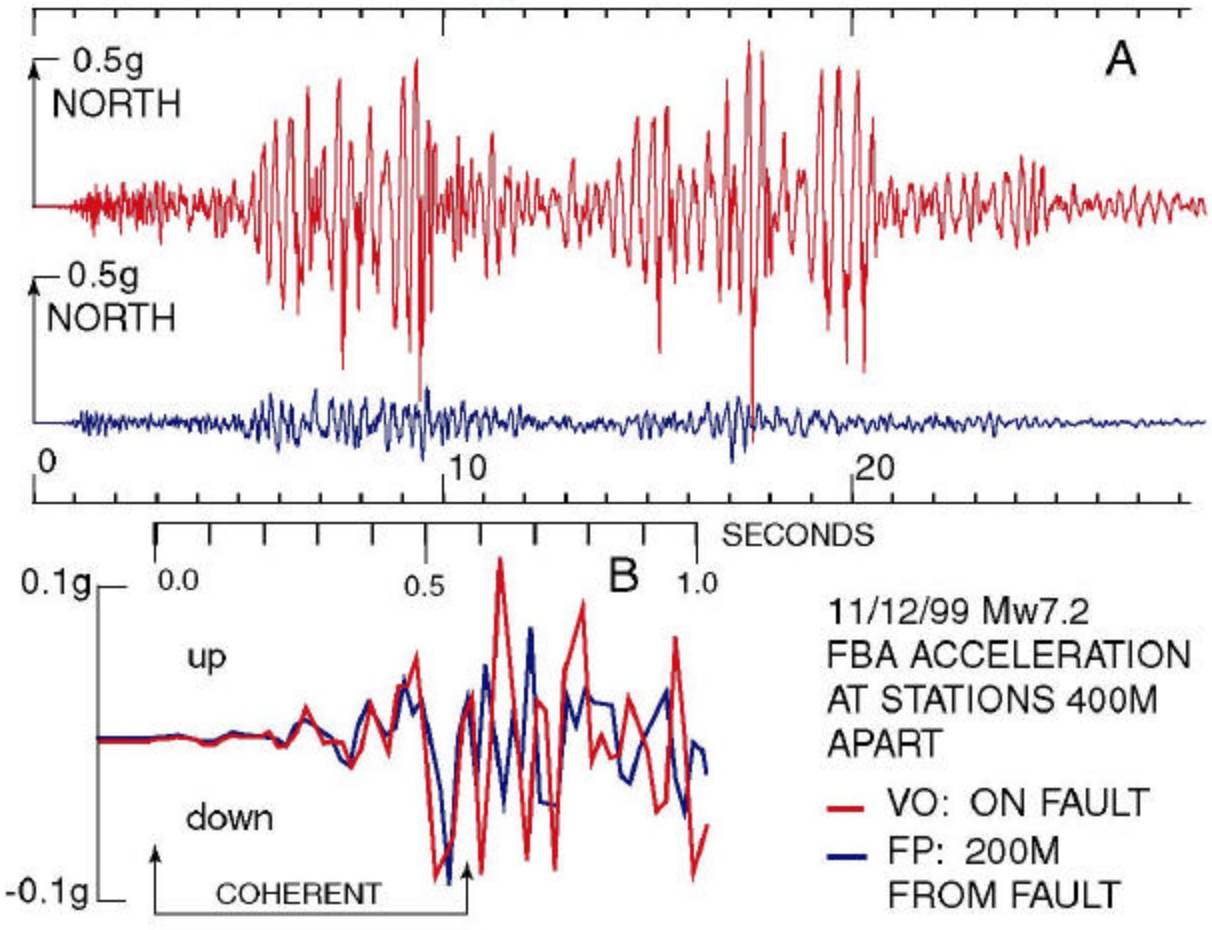

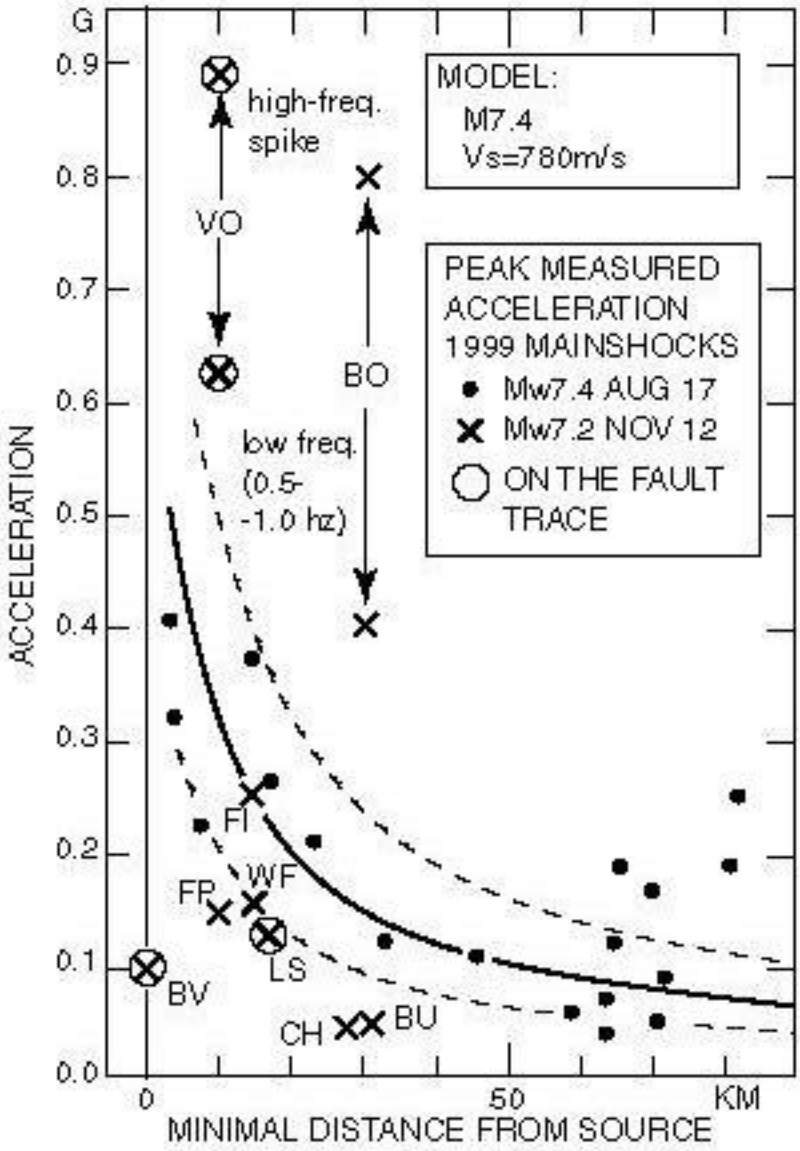

Figure 9. Peak acceleration versus closest distance from the source recorded by the Karadere network (except station BO near Bolu) for the Mw 7.2 November 12 mainshock (X) compared with peak acceleration recorded for the August 17 Mw 7.4 mainshock (•). Data from the main fault trace are circled. The model is for a Mw7.4 (Boore et al. 1997).

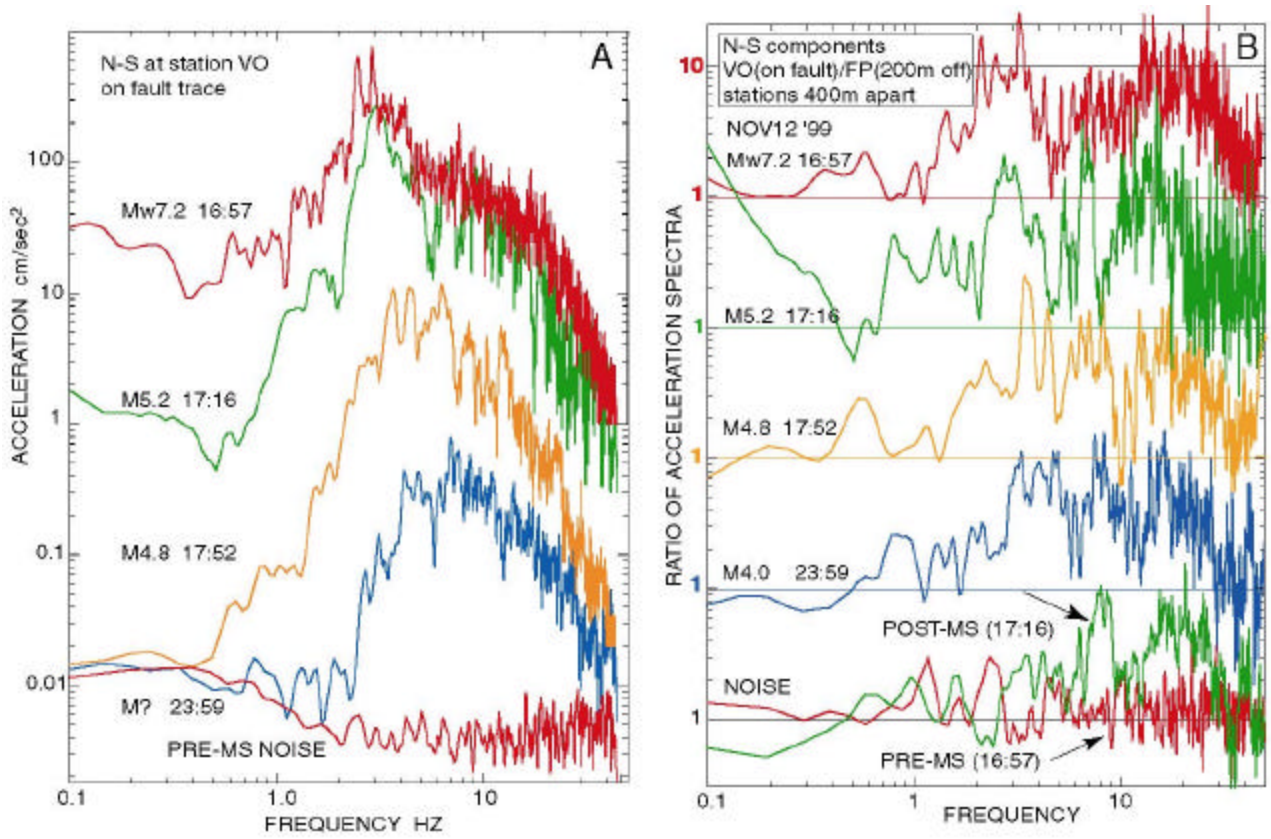

Figure 10A: Amplitude spectra of acceleration at station VO, N-S FBA component for the M7.2 Nov 12 '99 mainshock, three early aftershocks, and pre-mainshock noise. The four earthquakes span the size range M4-7.2. Station VO shows evidence of strong site amplification (Figure 8A). Note, however, that pre-mainshock noise is remarkably flat, particularly in the 1-10 hz frequency range. Note also that the M5.2 event 19 minutes after the mainshock has higher low-frequency energy than expected from a typical source model. B: Ratios of acceleration spectra for the N-S components at stations VO, on the trace of the August 17 rupture, and FP, 200m off this trace and 400m from VO. Spectral ratios are shown for the same four earthquakes and pre-mainshock noise sample as in A and for an additional noise sample 19 minutes after the Nov 12 '99 mainshock. The spectral ratios for the earthquakes show a broad peak centered at 2-3 seconds. The spectral ratio of this peak is 10 for the four events, but its frequency seems to decrease as ground motion increases. This peak is however not prominent in the spectral ratios for the noise, particularly before the mainshock.